

*Supporting information*

*for*

**Table-Salt Enabled Interface-Confined Synthesis of Covalent Organic  
Framework (COF) Nanosheets**

*Xiansong Shi, Dongwei Ma, Fang Xu, Zhe Zhang, and Yong Wang\**

State Key Laboratory of Materials-Oriented Chemical Engineering, and College of  
Chemical Engineering, Nanjing Tech University, Nanjing 211816, P. R. China

E-mail: yongwang@njtech.edu.cn

**Table of contents**

**1. EXPERIMENTAL SECTION**

**2. FIGURES AND TABLES**

**3. REFERENCES**

## 1. EXPERIMENTAL SECTION

### Materials

The big NaCl (*b*NaCl) particles were purchased from Xilong Scientific. Amine monomers including *p*-phenylenediamine (Pa, 97%) and benzidine (BD, 97%) were obtained from Aladdin. Aldehyde monomers, 1,3,5-triformylphloroglucinol (95%, Tp) and 1,3,5-triformylbenzene (95%, Tb), were purchased from TongChuangYuan Pharmaceutical (Sichuan, China) and YanShen Technology (Jilin, China), respectively. Acetic acid (AcOH) used as catalyst was purchased from Shanghai ShenBo Chemical. The monomer for the synthesis of boron-based CON, *p*-benzenediboronic acid (PB), was purchased from YanShen Technology (Jilin, China). Solvents including mesitylene, 1,4-dioxane (DOX) were obtained from Sinopharm Chemical Reagent and Shanghai LinFeng Chemical Reagent, respectively. Porous anodic aluminum oxide (AAO) substrates (2.5 cm, Whatman) with an average pore size of ~20 nm were used as supports for CON membrane preparation. Poly(vinylidene fluoride) (PVDF) microfiltration membranes (Millipore) with an average pore size of ~220 nm were served as substrates to support COF films grown on salt plates. Dyes including methyl blue (MB), acid fuchsin (AF), Eosin Y (EY, water soluble), and methyl Orange (MO) were obtained from Institute of Chemical Reagent (Tianjin, China), and Evans blue (EB) was purchased from Solarbio. All chemicals were used as received without further purification. Deionized water (DI water, conductivity: 8-20  $\mu\text{s cm}^{-1}$ , Wahaha Co.) was used in all the experiments.

## Methods

### Recrystallization of NaCl particles

The *b*NaCl particles with an average size of  $\sim 440$   $\mu\text{m}$  was dissolved in DI water to form a saturated solution. Then, excessive ethanol was added to the obtained solution to promote the recrystallization of NaCl crystals. The solution was then filtrated and dried under atmospheric conditions to yield recrystallized small NaCl (*s*NaCl) particles.

### Synthesis of imine-linked CONs

In a PTFE-lined autoclave with a capacity of 25 mL, 0.015 mmol of amine monomers (1.6 mg for Pa or 2.8 mg for BD) were dissolved in 10 mL mixed solvent containing 5 mL mesitylene and 5 mL DOX. Then, 100  $\mu\text{L}$  of 6 M AcOH was slowly added to the amine solution, which resulted in a homogeneous solution after ultrasonic treating at 100 W for 5 min. Then, 0.01 mmol of aldehyde monomers (2.1 mg for Tp or 1.6 mg for Tb) were added to the obtained solution to form a yellow precursor solution. Subsequently, the solution was immediately mixed with  $\sim 25$  g NaCl (*s*NaCl or *b*NaCl) particles followed by bubbling with nitrogen for 5 min. The as-obtained mixture in the autoclave was transferred to an oven to perform solvothermal synthesis at 120  $^{\circ}\text{C}$  for 3 days. After being cooled, the product was thoroughly washed with DOX and ethanol to remove the unreacted monomers and catalyst. The produced NaCl@CONs were then vacuum drying at 100  $^{\circ}\text{C}$  overnight before use.

### **Synthesis of imine-linked COF particulates**

Similar to the synthesis of CONs, 0.3 mmol of aldehyde monomers and 0.45 mmol of amine monomers were dissolved in 15 mL mixture containing 7.5 mL mesitylene and 7.5 mL DOX followed by adding of 150  $\mu$ L 6M AcOH. After bubbling with nitrogen for 5 min, the autoclave was then conducted with a solvothermal synthesis at 120 °C for 3 days. The obtained COF powders were thoroughly washed with DOX and ethanol, and vacuum drying at 100 °C overnight before further characterizations.

### **Synthesis of boron-based CONs (COF-1)**

Typically, 0.01mmol PB molecules were dissolved in 10 mL mixture containing 5 mL mesitylene and 5 mL DOX to form a precursor solution. About 25 g sNaCl crystals were added into the precursor solution after ultrasonic treatment under 100 W for 5 min. Subsequently, the mixture was heat-treated at 120 °C for 3 days to generate sNaCl@CON. After solvothermal synthesis, the obtained powders was thoroughly washed using DOX and ethanol and vacuum drying at 100 °C overnight.

### **Preparation of imine-linked CON membranes**

The vacuum-assisted filtration method was used to fabricate the multi-layered CON membranes. Because TpPa CONs can be easily released from salts by ultrasonic treatment, the preparation of TpPa membranes was conducted by directly filtrating released CONs on AAO supports. Specifically, designed dosages of sNaCl@TpPa ranging from 40 to 80 mg were firstly dispersed in ~30 g ethanol followed by treating under 300 W for 1 h, the obtained solution was then standing at room temperature for at least 3 h. Thus-prepared supernate was used for filtration to fabricate

TpPa-based membranes (Scheme S1). As for the preparation of TpBD membranes, a modified vacuum filtration was used because simple ultrasonic treatment can not release TpBD CONs from salts. Here, per 10 mg sNaCl@TpBD was firstly dispersed with 3 mL ethanol to generate a turbid liquid after ultrasonic treatment. Subsequently, 3 mL of the ethanol dispersion was filtrated through the substrate to produce a sNaCl@TpBD-AAO composite structure. Then, 2 mL of DI water was slowly filtrated through the membrane to remove salts and form a CON-stacked morphology. The two steps, deposition of sNaCl@CON powders and removal of salts, were cycled until the full use of the prepared dispersion (Scheme S2). Notably, the sNaCl@TpBD ethanolic solution was ultrasonically treated before every filtration process. After filtration of CONs on AAO supports, the CON-AAO membranes were filtrated with enough DI water again to completely remove salt particles and vacuum drying under 60 °C overnight.

### **Characterization**

The morphologies of the samples were studied using a field-emission scanning electron microscopy (SEM, Hitachi S-4800, Japan). The thickness of the CONs and films was analyzed by an atomic force microscopy (AFM, Park XE-100) in the noncontact mode, the samples were dropped on silicon wafers and dried at room temperature. The detailed morphologies of CONs was also examined using a field-emission high resolution transmission electron microscope (TEM, Tecnai G2 F30 S-Twin, FEI). The powder X-ray diffraction (XRD) patterns were obtained at room temperature using a Rigaku SmartLab X-ray diffractometer operating in the  $2\theta$  range

of 2-40° and at a scanning rate of 0.02° s<sup>-1</sup>. The fourier transform infrared spectra (FTIR) were determined using a spectrometer (Nicolet 8700) in the scanning range of 4000-600 cm<sup>-1</sup>. Thermogravimetric analysis (TGA) was performed on a Netzsch STA 409PC thermal analyzer in the temperature range of 25-700°C with a heating rate of 5 °Cmin<sup>-1</sup> in nitrogen to detect the thermal stability of thus-prepared CONs. Water contact angles of the substrates and CON-based membranes were performed on a contact angle goniometer (DropMeter A100, Maist).

### **Permeance and rejection tests**

In this work, all permeation tests were performed with the membrane covered with a 220-nm PVDF support from the top on a dead-end filtration cell (Amicon8003, Millipore) at 0.5 bar. As for permeance tests, precompaction of the membrane at the same pressure for 30 min was necessary to achieve a stabilized water permeance. The reported permeance was obtained from the average value of triplicate experimental results conducted with three different membranes. Water permeance ( $P$ , Lm<sup>-2</sup>h<sup>-1</sup>bar<sup>-1</sup>) was calculated by measuring permeate volume ( $\Delta V$ , L) per unit membrane area ( $A$ , m<sup>2</sup>) per unit time ( $t$ , h) per operated pressure ( $\Delta p$ , bar) according to the following equation:

$$P = \Delta V / (A t \Delta p)$$

Rejection performance of the produced membranes was performed by passing 25 ppm dye aqueous solution through the samples with stirring at 600 rpm. The initial 2 mL of the filtrate was discarded, and subsequent 2 mL was collected for the rejection analysis. Dye concentrations in feed, permeation, and retention were determined by

a UV-vis spectrometer (NanoDrop 2000c, Thermo Scientific). The rejection rates ( $R$ ) were calculated by the following equation:

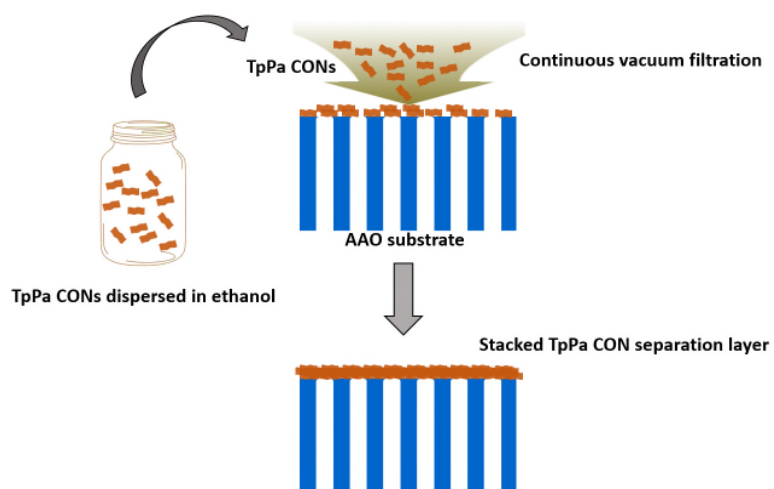
$$R=100 \times (1-C_p / C_f)$$

where  $C_p$  and  $C_f$  are dye concentrations in the permeation and the feed, respectively

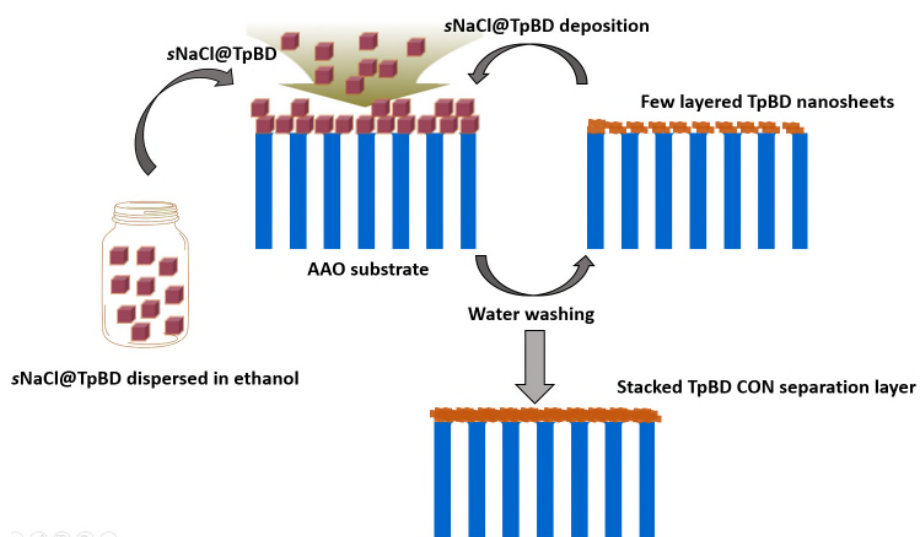
As for the separation of MO from MO and EB mixture, a 5 mL of feed, mixed by 2.5 mL, 25 ppm dye solution of EB and MO, respectively, was charged to the dead-end cell with stirring at 600 rpm. The obtained solutions of feed, permeation, and retention were also analyzed using a UV-vis spectrometer.

The long-term stability of the membrane was investigated by a continuous filtrating of 25 ppm EB aqueous solution for 30 h. The dye solution permeance and rejection were also calculated *via* above-mentioned two equations, respectively.

## 2. FIGURES AND TABLES



**Scheme S1** The fabrication process of TpPa CON membranes.



**Scheme S2** The fabrication process of TpBD CON membranes.



**Fig. S1** Digital image of the PTFE container showing the salt-confined environment during the synthesis of TpPa CONs. In the synthesis system, excessive salt particles were added into the autoclave to create copious confined solid-liquid interfaces. The monomer solution was totally confined in the space among the salt particles.

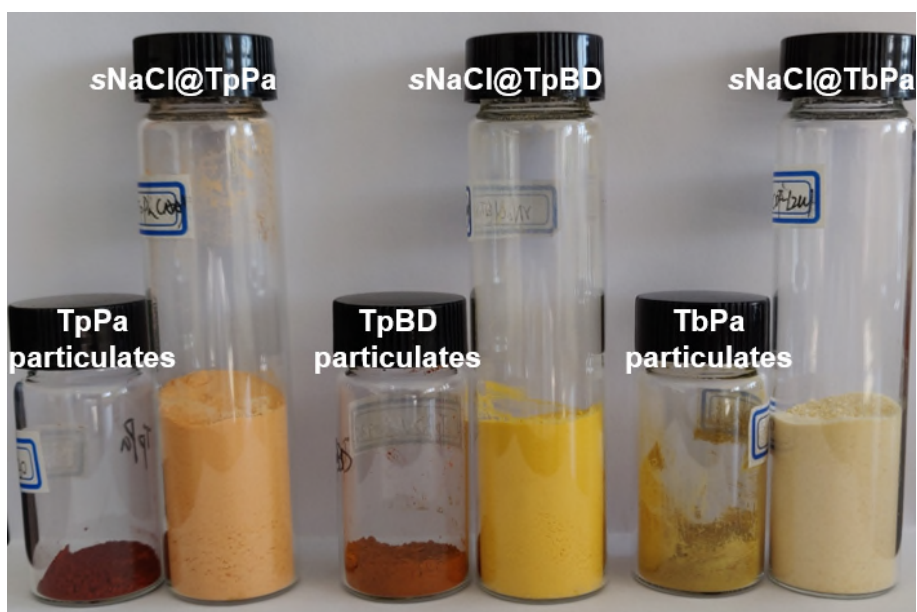


**Fig. S2** Digital images of COF particulates synthesized in the absence of salts and CONs synthesized in the presence of salts. Here, the amount of monomer pairs for the synthesis of COF particulates was 30 times higher than that of corresponding CONs.

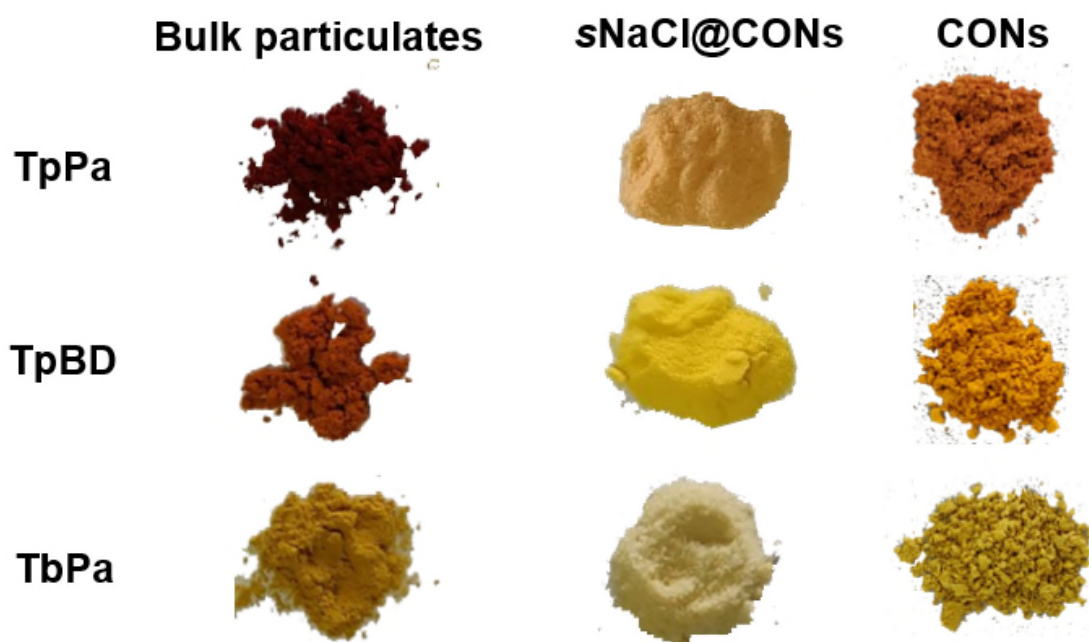


Fig. S3 Digital images of COF particulates, sNaCl@CONS, and CONS.

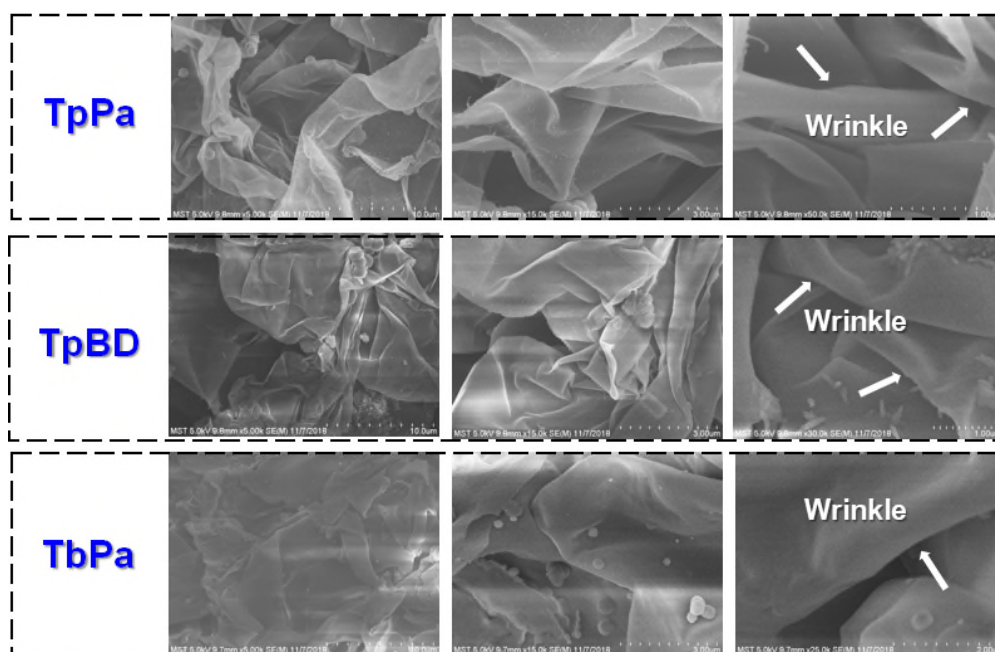
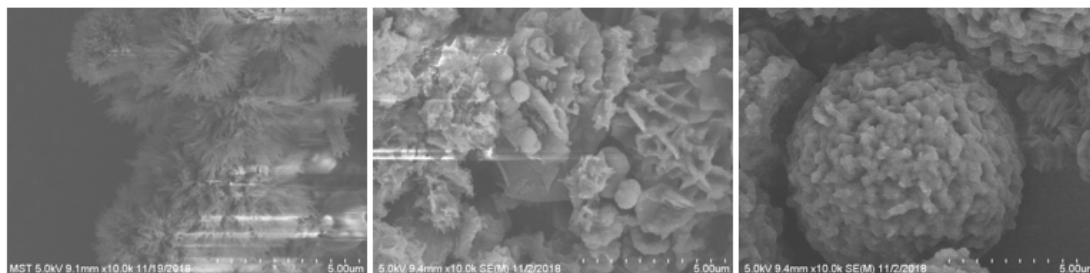


Fig. S4 SEM images of CONS after washing away the salts.

TpPa

TpBD

TbPa



**Fig. S5** SEM images of COF particulates produced by traditional solvothermal synthesis without salts. The traditional solvothermal synthesis can only produce aggregated particulates, which are totally different from the sheet-like structures prepared with salts.

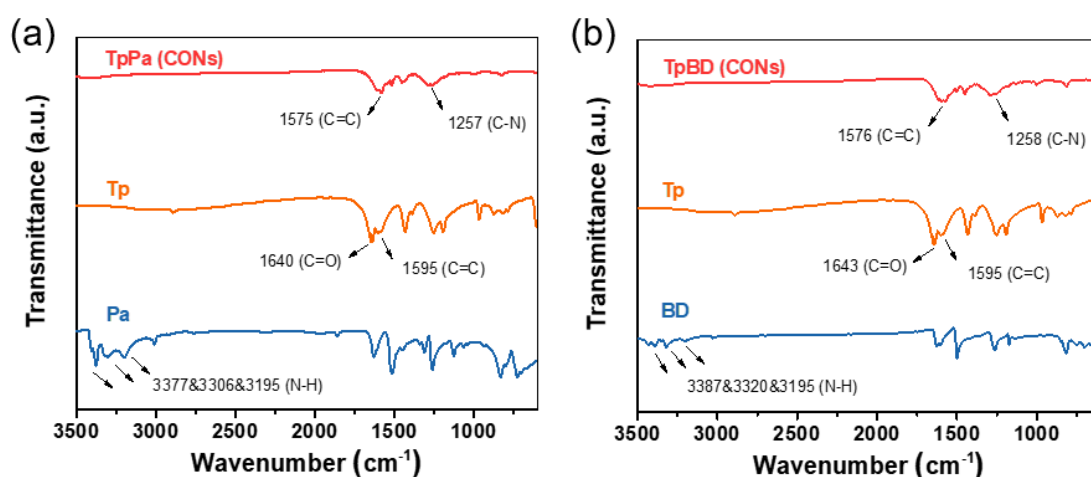


**Fig. S6** FTIR spectra of CONs and corresponding monomers. (a) TpPa, (b) TpBD. The disappearance of  $-N-H$  and aldehyde  $-C=O$  stretching bands demonstrated a complete consumption of monomer pairs.

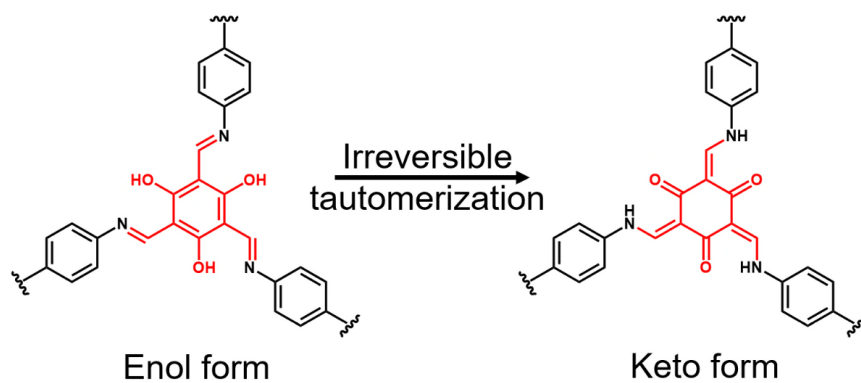


**Fig. S7** The irreversible enol-to-keto tautomerization.

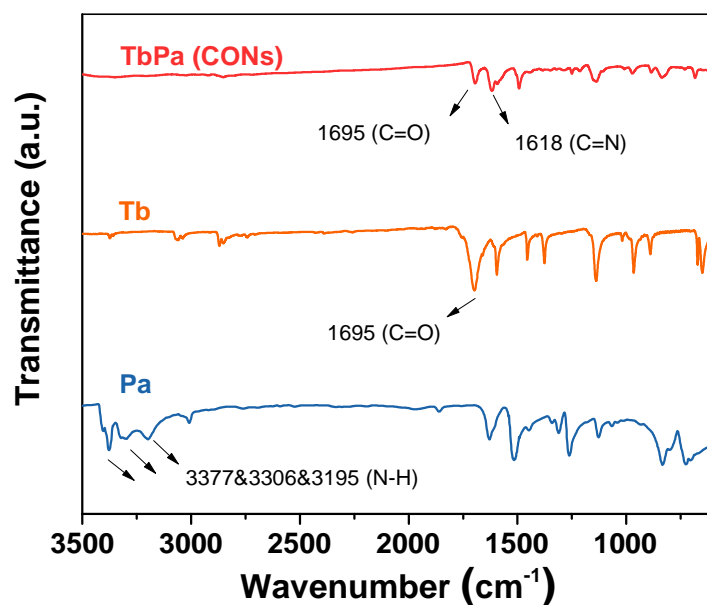


**Fig. S8** FTIR spectrum of TbPa CONs and corresponding monomers. The greatly reduced intensities of  $-N-H$  and aldehyde  $-C=O$  bonds confirmed the formation of imine bonds during synthesis.

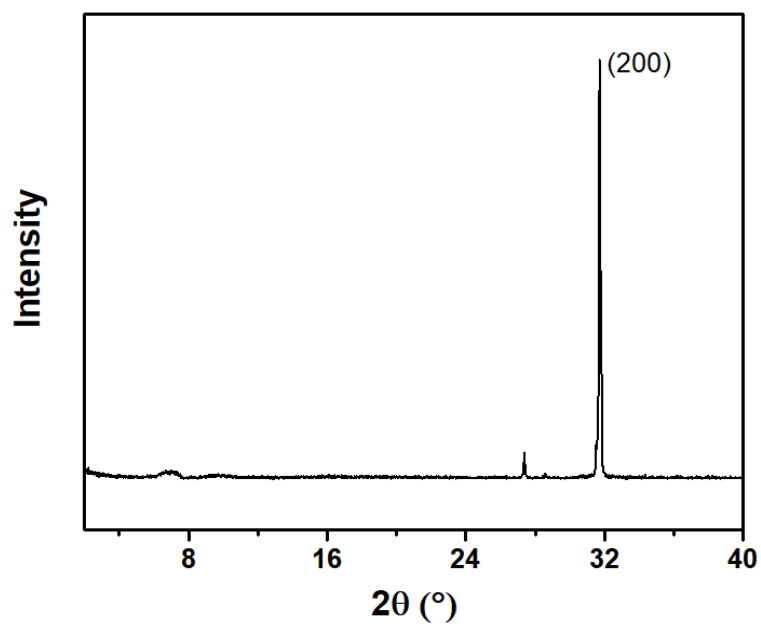


**Fig. S9** The XRD pattern of sNaCl@TpPa.

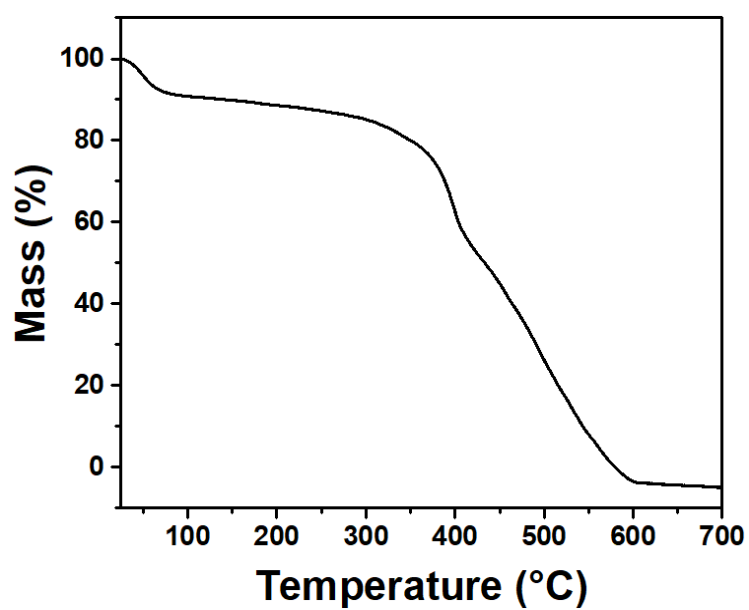


**Fig. S10** The TGA data of TpPa CONs under N<sub>2</sub> atmosphere.

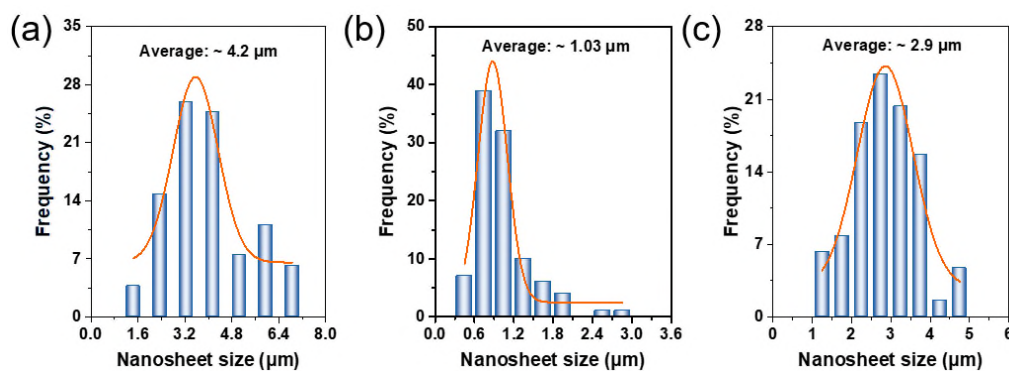


**Fig. S11** Lateral size distribution of imine-linked CONs. (a) TpPa, (b) TpBD, (c) TbPa.

The lateral size distribution of CONs was obtained by measuring at least 100 nanosheets.

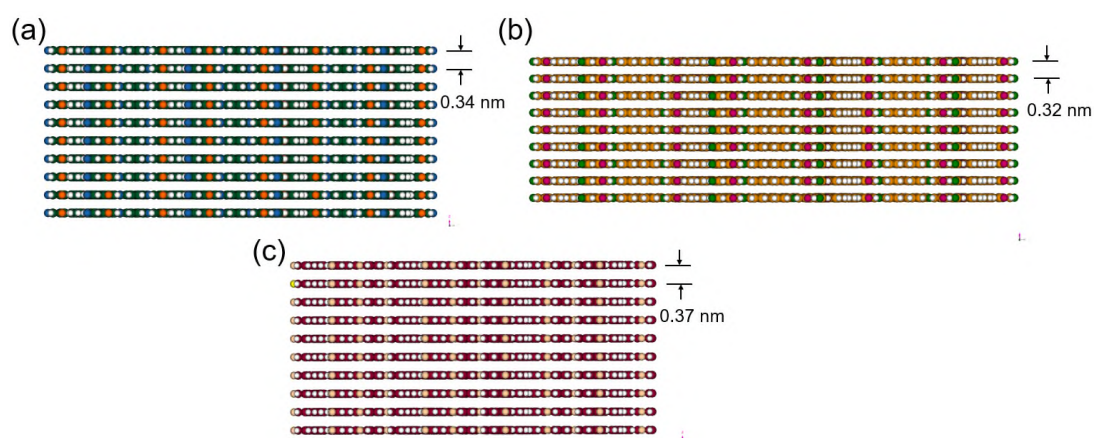


**Fig. S12** Simulated structures of CONs showing 10 layers. (a) TpPa, (b) TpBD, (c) TbPa.

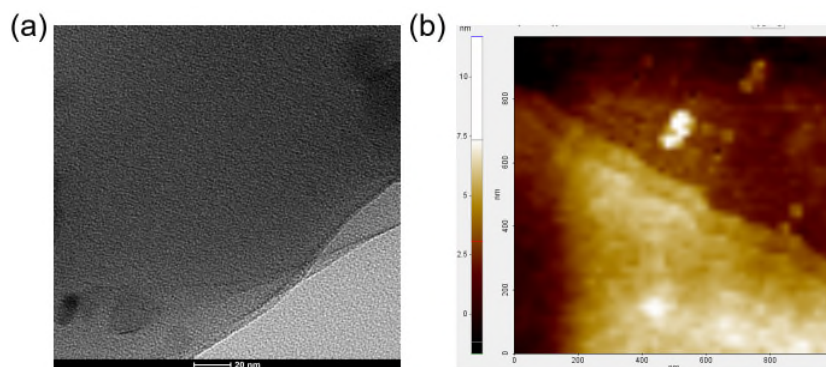


**Fig. S13** TEM (a) and AFM (b) images of TpPa CONs. The stacking layered structure of CONs was clearly shown in these two images.



**Fig. S14** Digital images of CONs dispersed in ethanol. After dispersion, the solution showed a strong Tyndall effect, demonstrating the presence of CONs. The prepared CON dispersion maintained stable in ambience for at least one week.

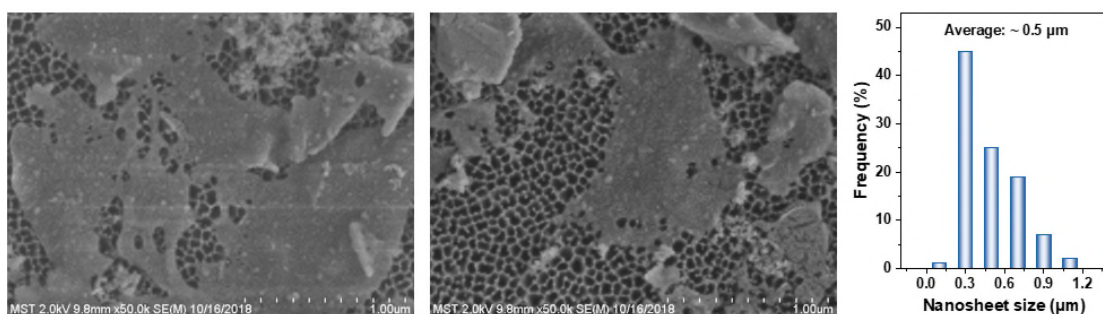


**Fig. S15** SEM images and lateral size distribution of COF-1 nanosheets.

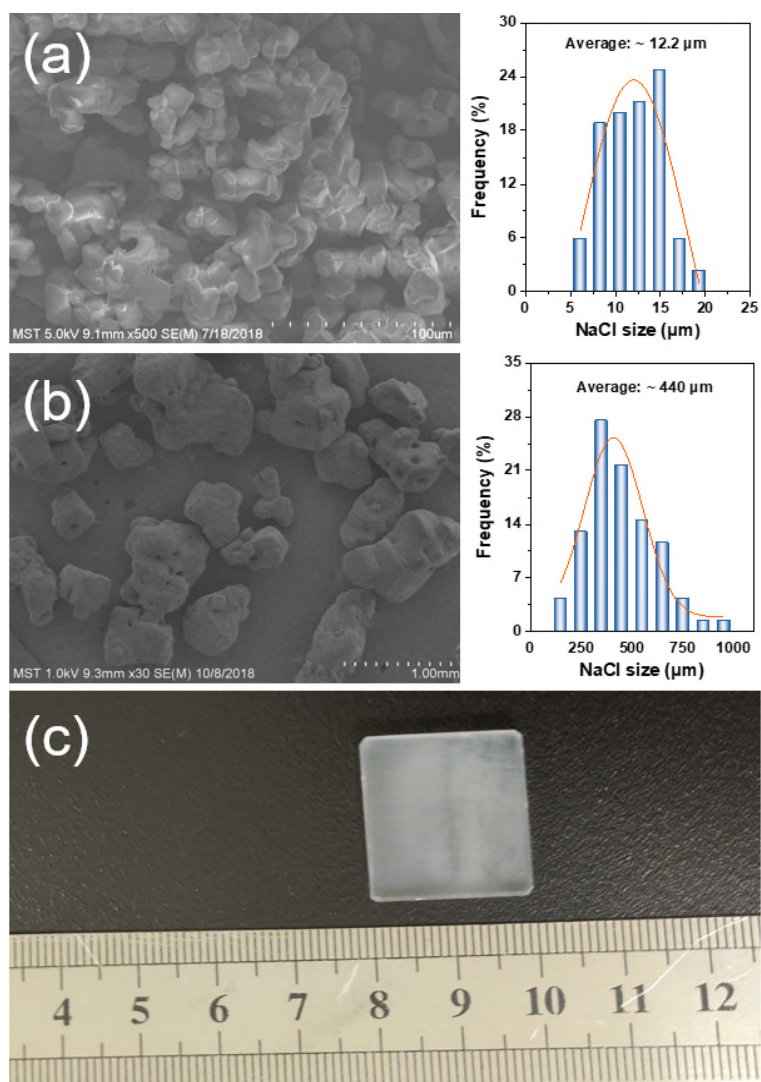


**Fig. S16** SEM images and corresponding lateral size distributions of salt substrates with different sizes: *sNaCl* (a), and *bNaCl* (b), and digital image of a NaCl plate (c).

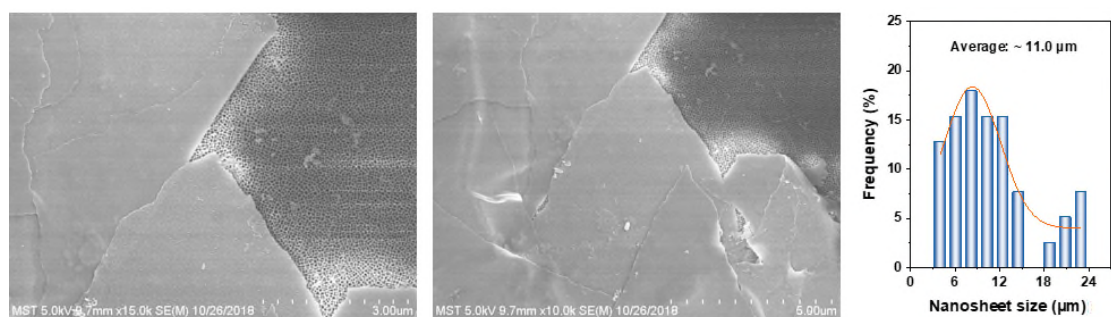


**Fig. S17** SEM images and corresponding lateral size distribution of TpPa nanosheets released from *bNaCl* particles.

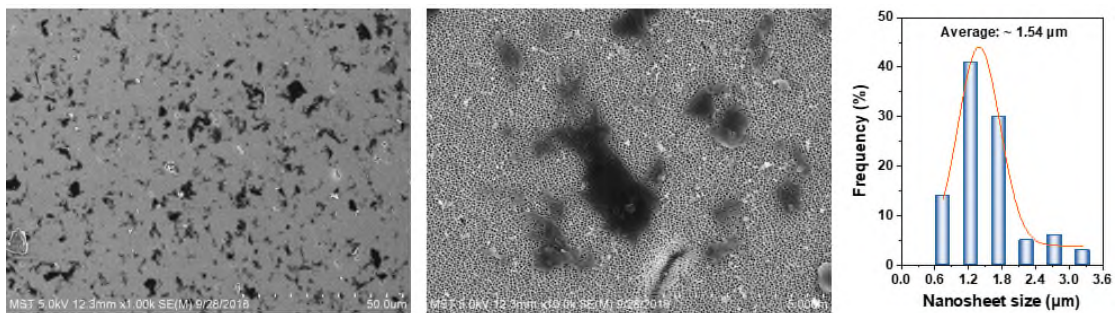


**Fig. S18** SEM images and corresponding lateral size distribution of TpBD nanosheets released from *b*NaCl particles.

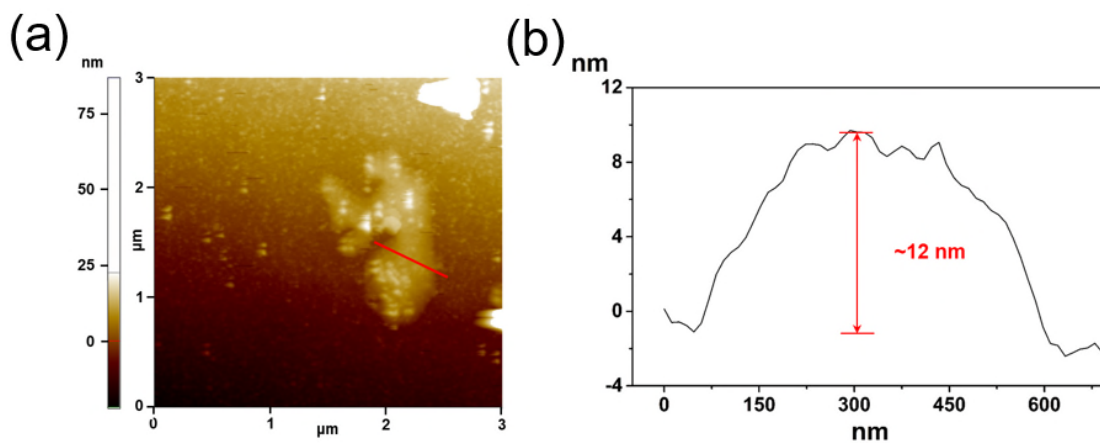


**Fig. S19** The AFM image (a) and corresponding height profile (b) of TpBD nanosheets released from *b*NaCl particles.

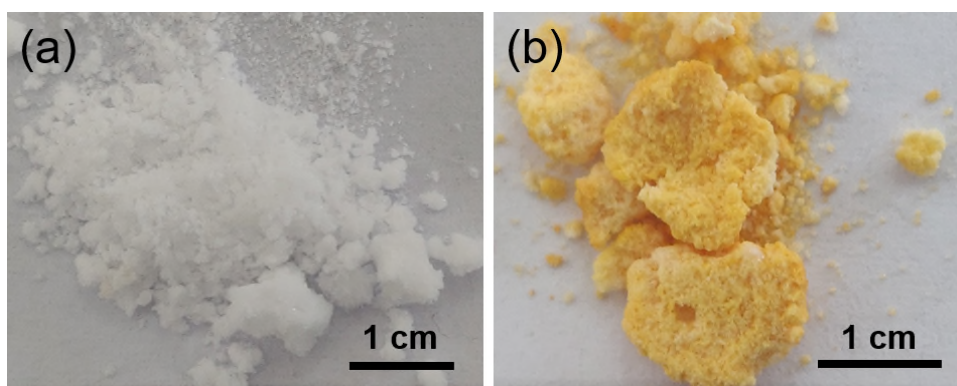


**Fig. S20** Digital images of stacked sNaCl particles before (a) and after synthesizing for 5 min (b).

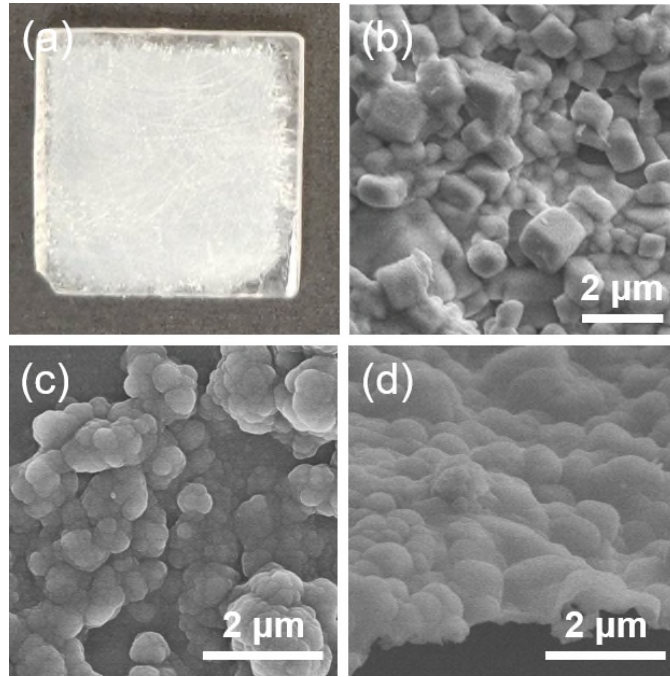


**Fig. S21** Characterization of CONs grown on a salt plate with rough surfaces. (a) the photograph of the rough NaCl plate, (b) the SEM image showing the rough surface of the plate, (c) the SEM image of the surface of CON grown on the salt plate, (d) the SEM image showing the cross-sectional morphology of CONs released from the salt plate.

**Table S1** The caculated surface areas of NaCl salts with different sizes.

Type	Size	Surface area (cm <sup>2</sup> )
Small NaCl	12.2 μm	56557
Big NaCl	440 μm	1568
Salt plate	2 cm×2 cm×0.3 cm	10.4

$$v=m/\rho \quad (1)$$

where  $v$  (cm<sup>3</sup>) is the volume of salts,  $m$  (g) is the mass of salts (25 g),  $\rho$  (g cm<sup>-3</sup>) is the

density of NaCl ( $2.165 \text{ g cm}^{-3}$ ).

We consider that both the small and big salt are in the six cubic structure. According to Equation (1),  $v$  is calculated to be  $11.5 \text{ cm}^3$ . As the average sizes of small and big salt particles are  $12.2$  and  $440 \text{ }\mu\text{m}$ , respectively. Thus the surface areas of  $s\text{NaCl}$  and  $b\text{NaCl}$  are calculated to be  $56557$ , and  $1568 \text{ cm}^2$ , respectively. The surface area of NaCl plate is calculated to be  $10.4 \text{ cm}^2$  based on its size.

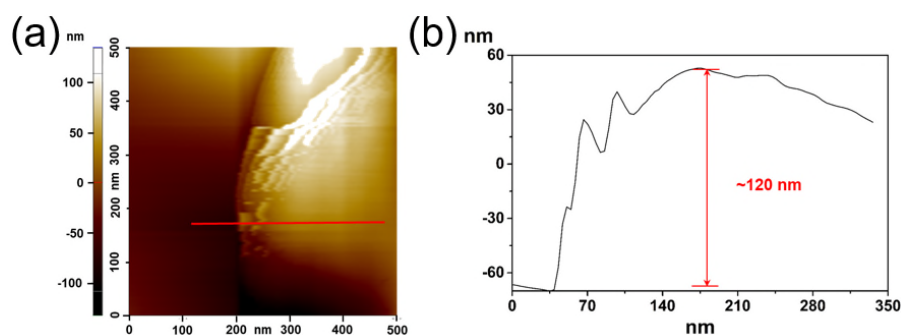


**Fig. S22** The AFM image of the TpBD film released from the NaCl plate. the AFM image (a) and corresponding height profile (b).

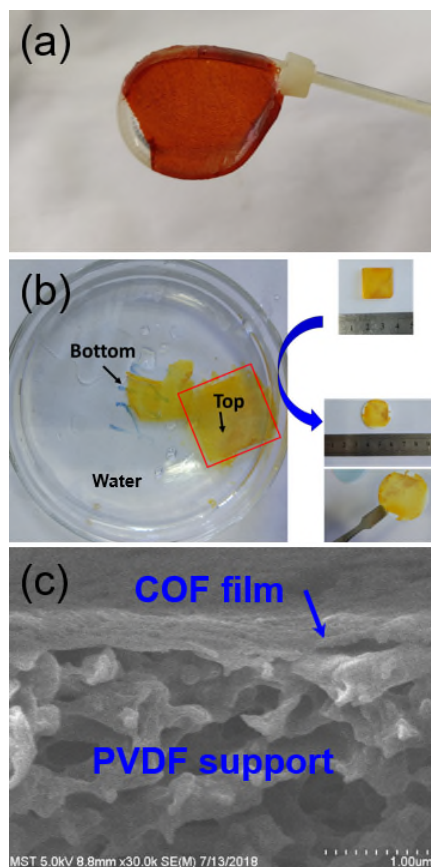
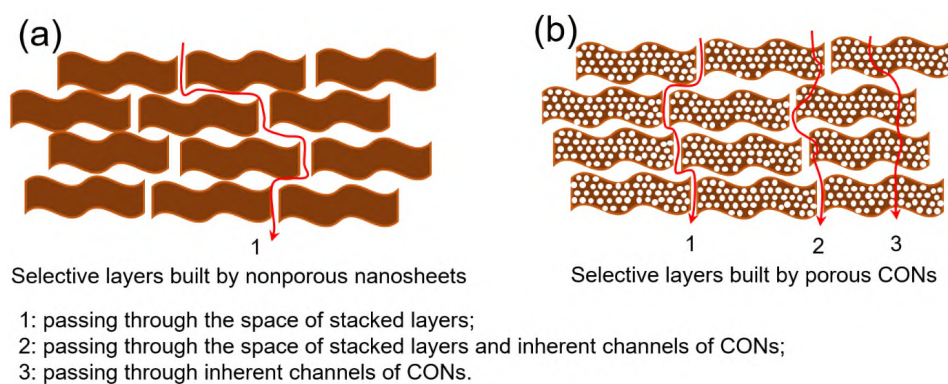


**Fig. S23** Images of COF films grown on the salt plate transferred to different substrates. (a) The TpPa film transferred onto a plastic ring, (b) the TpBD film transferred onto a PVDF support, and (c) the cross-sectional SEM image of TpPa film supported by a PVDF support.



**Scheme S3** Schematic illustration of possible transporting ways through the selective built by nonporous nanosheets (a) and porous CONs (b).



**Fig. S24** Digital image of the home-made vacuum filtration setup.

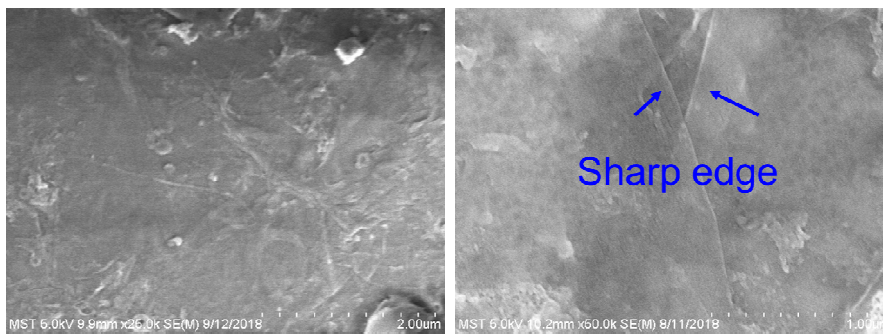


**Fig. S25** Surface morphologies of the TpBD-AAO membrane. Under a high magnification, sharp edges can be clearly observed, indicating the successful formation of stacked CONs.

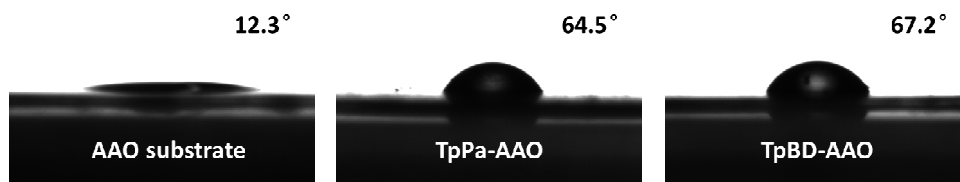


**Fig. S26** Water contact angles of AAO substrate (a), TpPa-AAO (b), and TpBD-AAO (c).

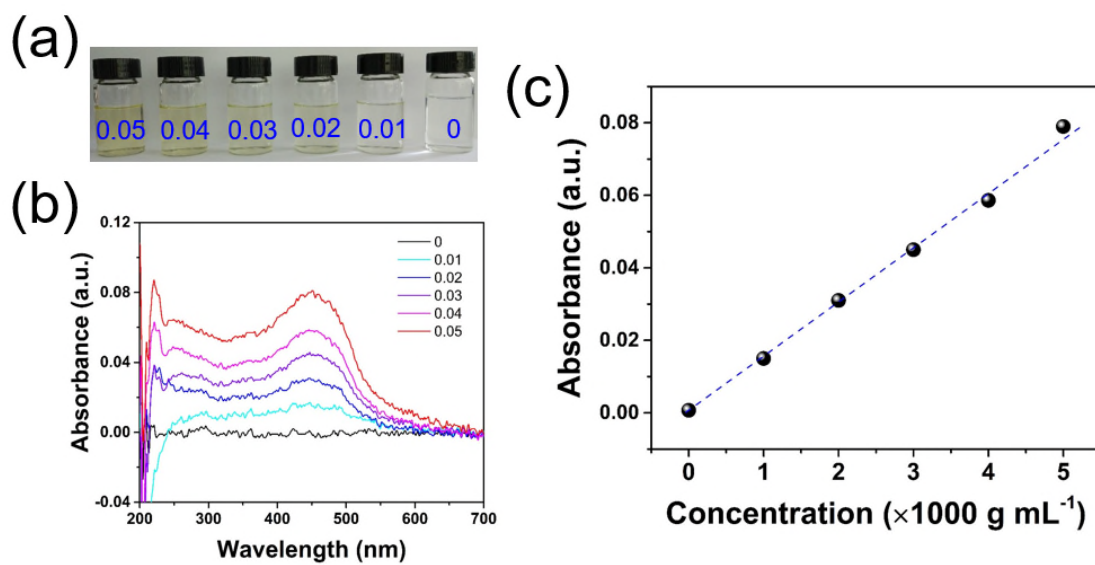


**Fig. S27** The relationship between the amount of TpBD CONs released from sNaCl particles and the absorbance tested using a UV-vis spectrometer. (a) Physical appearance of the CON solutions with the amount of sNaCl@TpBD ranging from 0 to 0.05 g; (b) the UV-vis spectra of CON solutions; (c) the relationship between CON concentration and absorbance.

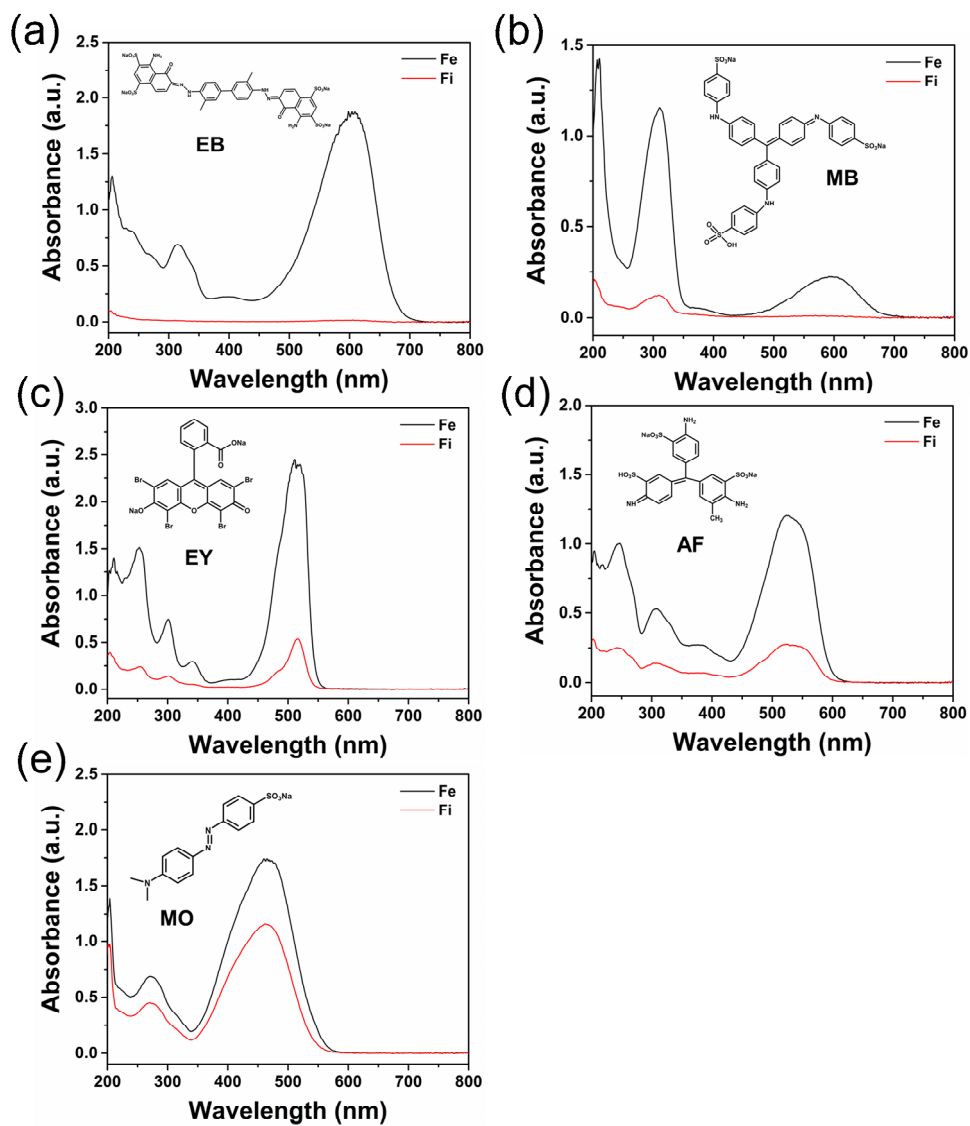


**Fig. S28** UV-vis spectra of the feed (Fe) and filtrate (Fi) in the rejection tests of five different dyes.

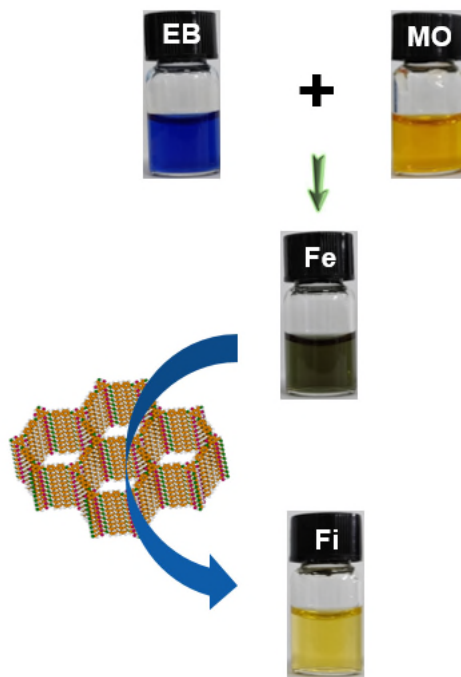


**Fig. S29** The color change of solutions during the filtration.

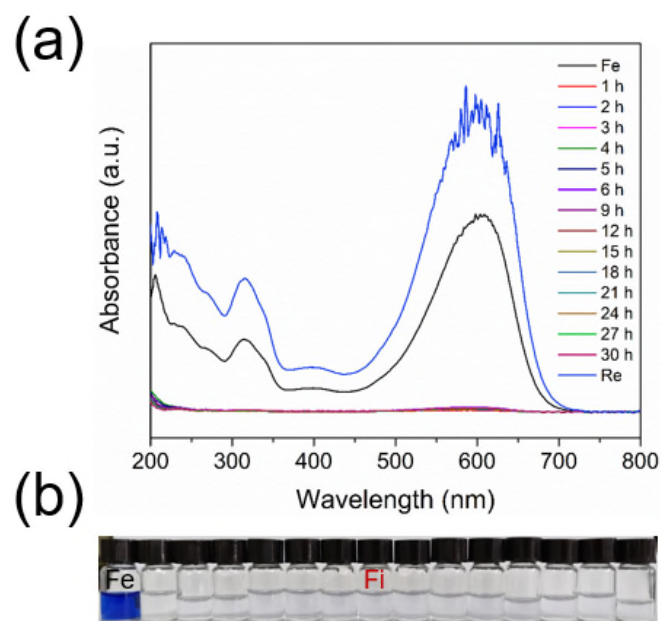


**Fig. S30** The UV-vis spectra (a) and the change in solution color (b) during long-term filtration tests for 30 h.

**Table S2** Comparison of dye removal performance of membranes prepared by different methods.

Membranes	Dye molecules	Permeance (Lm <sup>-2</sup> h <sup>-1</sup> bar <sup>-1</sup> )	Rejection (%)	Reference
ZIF-8/PSS	Methyl blue	26.5	98.6	S1
CMCNa/PP	Methyl blue	0.87	99.75	S2
ZIF-12/PAN	Methyl blue	27.2	99.4	S3
PEI/CMCNa/PP	Congo red	5.7	99.4	S4
ZIF-8/PES	Rose bengal	1.3	98.95	S5
COF/PSf	Congo red	50	99.5	S6
ZIF-8/PEI/PAN	Congo red	78	99.2	S7
TA/GOQDs/PAN	Congo red	11.67	99.8	S8
uGNM/AAO	Methyl blue	21.8	99.2	S9
g-C <sub>3</sub> N <sub>4</sub> /AAO	Evans blue	11.6	90	S10
TpPa <sub>80</sub> /AAO	Evans blue	121.8	99.2	This work
TpBD <sub>80</sub> /AAO	Evans blue	88.9	99.2	This work

### 3. REFERENCES

S1 R. Zhang, S. Ji, N. Wang, L. Wang, G. Zhang, J.R. Li, Coordination-driven in situ self-assembly strategy for the preparation of metal-organic framework Hybrid Membranes, *Angew. Chem. Int. Ed. Engl.*, 53 (2014) 9775-9779.

S2 S. Yu, Z. Chen, Q. Cheng, Z. Lü, M. Liu, C. Gao, Application of thin-film composite hollow fiber membrane to submerged nanofiltration of anionic dye aqueous solutions, *Sep. Purif. Technol.*, 88 (2012) 121-129.

S3 N.X. Wang, X.T. Li, L. Wang, L.L. Zhang, G.J. Zhang, S.L. Ji, Nanoconfined zeolitic imidazolate framework membranes with composite layers of nearly zero thickness, *ACS Appl. Mater. Interfaces*, 8 (2016) 21979-21983.

S4 Q. Chen, P. Yu, W. Huang, S. Yu, M. Liu, C. Gao, High-flux composite hollow fiber nanofiltration membranes fabricated through layer-by-layer deposition of oppositely charged crosslinked polyelectrolytes for dye removal, *J. Membr. Sci.*, 492 (2015) 312-321.

S5 Y. Li, L.H. Wee, A. Volodin, J.A. Martens, I.F. Vankelecom, Polymer supported ZIF-8 membranes prepared via an interfacial synthesis method, *Chem. Commun.*, 51 (2015) 918-920.

S6 R. Wang, X. Shi, A. Xiao, W. Zhou, Y. Wang, Interfacial polymerization of covalent organic frameworks (COFs) on polymeric substrates for molecular separations, *J. Membr. Sci.*, 566 (2018) 197-204.

S7 L. Yang, Z. Wang, J. Zhang, Highly permeable zeolite imidazolate framework composite membranes fabricated via a chelation-assisted interfacial reaction, *J.*

*Mater. Chem. A*, 5 (2017) 15342-15355.

S8 C. Zhang, K. Wei, W. Zhang, Y. Bai, Y. Sun, J. Gu, Graphene oxide quantum dots incorporated into a thin film nanocomposite membrane with high flux and antifouling properties for low-pressure nanofiltration, *ACS Appl. Mater. Interfaces*, 9 (2017) 11082-11094.

S9 Y. Han, Z. Xu, C. Gao, Ultrathin graphene nanofiltration membrane for water purification, *Adv. Funct. Mater.*, 23 (2013) 3693-3700.

S10 Y. Wang, L. Li, Y. Wei, J. Xue, H. Chen, L. Ding, J. Caro, H. Wang, Water transport with ultralow friction through partially exfoliated *g*-C<sub>3</sub>N<sub>4</sub> nanosheet membranes with self-supporting spacers, *Angew. Chem. Int. Ed. Engl.*, 56 (2017) 8974-8980.